IMA Journal of Applied Mathematics (2016) **81**, 522–537
doi:10.1093/imamat/hxw031
Advance Access publication on 14 July 2016

Thixotropy in yield stress fluids as a limit of viscoelasticity

MICHAEL RENARDY* AND YURIKO RENARDY
Department of Mathematics, 460 McBryde Hall, Virginia Tech, 225 Stanger St, Blacksburg, VA 24061-0123, USA
*Corresponding author: renardym@aol.com

[Received on 30 December 2014; revised on 24 February 2016]

Thixotropic yield stress fluids have a yield stress and viscosity which change slowly over time as the fluid undergoes structural changes. This article reviews recent work which shows how such behaviour can arise as a limit of viscoelastic flow when a relaxation time becomes large. The large relaxation time introduces a small parameter which can be used as a basis for singular perturbation studies. A simple prototype for a viscoelastic model will be used to illustrate the analysis. We review the behaviour in startup of shear flow, oscillatory shear flow and elongational flow and identify potential directions for future research.

Keywords: yield stress, thixotropy, viscoelastic fluids.

1. Introduction

Complex fluids such as polymers, pastes, suspensions and colloids show behaviour intermediate between fluids and solids. Traditionally, one distinguishes yield stress fluids, in which fluid versus solid behaviour depends on the magnitude of stress, and viscoelastic fluids, in which fluid versus solid behaviour depends on time scales. Yield stress fluids will start flowing only if the applied stress exceeds a critical value. Simple models for yield stress fluids are typically formulated in terms of generalized Newtonian models such as the Bingham or Herschel–Bulkley model.

However, for many complex fluids solid versus liquid behaviour depends on both time scales and the magnitude of stress. They show phenomena which place them well outside the realm of Bingham-like models. For instance, stress overshoots are common, see e.g. Nguyen & Boger (1992). Hysteresis has been observed, i.e. fluids 'unyield' at a much lower stress than the stress at which they yield (Coussot & Gaulard, 2005; James *et al.*, 1987). The hysteresis leads to coexistence of yielded and unyielded phases at the same stress and to shear banding (see e.g. Møller *et al.*, 2006). Moreover, the value of yield stress may depend on the time of observation; 'slow yielding occurs at lower values of stress than 'fast yielding (Caton & Baravian, 2008; Cheng, 1986; Stokes & Telford, 2004). We refer to Barnes (1999), Nguyen & Boger (1992), Coussot (2014) and Mewis & Wagner (2013) for reviews of the literature on yield stress fluids.

A typical example of 'delayed' yielding is shown in the data on ketchup displayed in Fig. 1. Here the fluid starts from rest, and after time $t = 0$ a constant shear stress is imposed. For sufficiently high stress, the fluid yields immediately. At low stresses, unyielded behaviour is observed. In between, however, there is a range of stresses in which yielding occurs at a time which increases with decreasing stress. Once yielding has occurred, many yield stress fluids remain in a yielded state long after motion has ceased. This is referred to as 'thixotropy.'

There are a number of theoretical efforts to explain more complex yield behaviour than provided by Bingham-like models. A popular approach starts from simple yield stress models such as Bingham or Herschel–Bulkley and introduces some kind of structural variable on which for instance the viscosity,

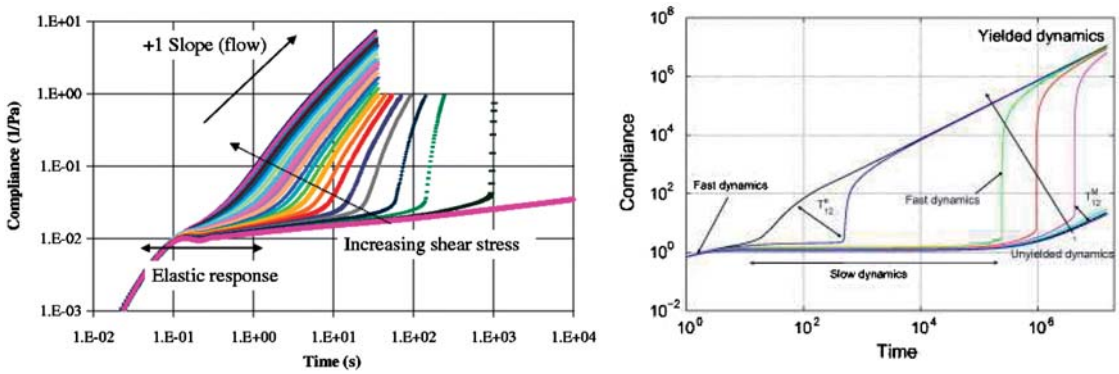

FIG. 1. Left: Observations of delayed yielding in ketchup (reproduced from Caton & Baravian (2008)). Right: Fit of these data using a modified PEC model (reproduced from Maki & Renardy (2012)).

yield stress or power law exponent may depend (Fielding, 2009; Picard *et al.*, 2002). An evolution equation is then postulated for the structure parameter. On the other hand, one may try to obtain complex yield stress behaviour as a limit of viscoelastic behaviour when a relaxation time becomes very large. In this point of view, there is no true yield stress, but yield stress behaviour arises in a singular limit where the relaxation time tends to infinity. This point of view was advocated in Barnes & Walters (1985). This article reviews recent work on the systematic use of asymptotics to analyse the large relaxation time limit of a viscoelastic model which is able to produce thixotropic yield stress behaviour. This approach was developed in recent work by Renardy (2010). He showed that the 'partially extending strand convection' (PEC) model of Larson (1984) is capable of explaining the salient features of thixotropic yield stress fluids. Larson obtained his model from a molecular theory of entangled polymers. The model has recently also been applied to wormlike micelles (Zhou *et al.*, 2008). Wormlike micelles are surfactant solutions which include such popular household items as shampoo. They are often viewed as 'apparent' yield stress fluids. In these fluids, the viscosity in the unyielded phase is two or three orders of magnitude higher than in the yielded phase, but is still small enough to observe a flow.

In Renardy (2010), the PEC model is formulated as a modification of the upper- convected Maxwell model which includes a 'microstructural parameter.' The model is described in terms of a conformation tensor $\mathbf{C}$, which satisfies a differential equation of the form

$$\mathbf{C}^{\nabla} + \lambda(\phi(\operatorname{tr}\mathbf{C})\mathbf{C} - \chi(\operatorname{tr}\mathbf{C})\mathbf{I}) = 0. \tag{1.1}$$

Here $\mathbf{C}^{\nabla}$ denotes the upper-convected time derivative given by

$$\mathbf{C}^{\nabla} = \frac{\partial \mathbf{C}}{\partial t} + (\mathbf{v}\cdot\nabla)\mathbf{C} - (\nabla\mathbf{v})\mathbf{C} - \mathbf{C}(\nabla\mathbf{v})^{T}, \tag{1.2}$$

where $\mathbf{v}$ is the velocity of the fluid. The constant λ has the dimension of inverse time, and is assumed to be small in a sense made precise below. The stress tensor $\mathbf{T}$ is related to $\mathbf{C}$ by

$$\mathbf{T}_{\mathrm{PEC}} = \psi(\operatorname{tr}\mathbf{C})\mathbf{C}. \tag{1.3}$$

If the functions ϕ, ψ and χ are constant, this model reduces to the upper-convected Maxwell model. In a thixotropic yield stress fluid, on the other hand, we should expect the viscosity and relaxation time to

decrease when the fluid yields; this is built into the model via the dependence on $\operatorname{tr}\mathbf{C}$. The trace of the conformation tensor thus fulfils the role of a microstructural parameter.

Let $s = \operatorname{tr}\mathbf{C}$. Larson's PEC theory leads to the model functions $\phi(s) = \chi(s) = s + \alpha$, $\psi(s) = k/(s+\alpha)$, where k is a stress modulus and $\alpha > -3$ is a dimensionless constant. Larson's molecular theory would lead to $\alpha \geq 0$. However, the only mathematical constraint that needs to be imposed on the model is the $s+\alpha$ should remain positive, and it can be shown that s always remains greater or equal to 3. We note that $s = \operatorname{tr}\mathbf{C}$ is equal to 3 in equilibrium where $\mathbf{C} = \mathbf{I}$.

The PEC model leads to a yield stress because, due to the term $s+\alpha$ in the denominator of ψ, the magnitude of $\mathbf{T}_{\text{PEC}}$ as given by (1.3) cannot exceed a threshold value. To account for the response of the fluid after yielding, we augment the PEC model by a Newtonian viscous term. Thus the total stress will be given by

$$\mathbf{T} = \psi(\operatorname{tr}\mathbf{C})\mathbf{C} + \eta(\nabla\mathbf{v} + (\nabla\mathbf{v})^T). \tag{1.4}$$

We can non-dimensionalize the model by scaling stresses with k and time with η/k. After redefining the stress as $\mathbf{T}/k$ and time as tk/η, we can and shall therefore set k and η equal to 1. The PEC model then has two dimensionless constants left: α and $\epsilon = \lambda\eta/k$, which we assume to be small. Both parameters have a natural physical interpretation. The ratio of yielded to unyielded viscosity, or equivalently, the ratio of the retardation time $\eta(3+\alpha)/k$ to the relaxation time $1/((3+\alpha)\lambda$, is $\epsilon(3+\alpha)^2$. The parameter α is related to the magnitude of the yield stress relative to the shear modulus: in 'fast' yielding (see the section on shear flows below), the ratio of yield stress to stress modulus is $\sqrt{3+\alpha}/2$. Thus a large value of α corresponds to a high yield stress, while a value close to -3 corresponds to a low yield stress.

We view the PEC model as a prototype of a theory which can explain thixotropic behaviour as a limit of viscoelasticity. The small number of parameters makes the model relatively simple, which allows a quite explicit analysis of a number of time-dependent flows in the limit of small ϵ. This paper will review results obtained by the authors along those lines over the last few years, including startup and cessation of shear flow (Maki & Renardy, 2010, 2012; Renardy, 2010), oscillatory shear flow (Renardy & Wang, 2015) and elongational flow (Grant & Renardy, 2015; Renardy & Grant, 2013).

2. Shear flows

In a shear flow, we have $\mathbf{v} = (u(y), 0, 0)$. In this case the PEC model reduces to $C_{22} = C_{33} = 1$, $C_{13} = C_{23} = 0$, and the remaining components of the conformation tensor satisfy the system

$$\begin{aligned} \dot{C}_{11} &= 2\kappa C_{12} - \epsilon(s+\alpha)(C_{11}-1), \\ \dot{C}_{12} &= \kappa - \epsilon(s+\alpha)C_{12}. \end{aligned} \tag{2.1}$$

Here $\kappa = u'(y)$ is the shear rate and $s = \operatorname{tr}\mathbf{C} = C_{11} + 2$. Under the assumption of creeping flow, we have

$$\frac{C_{12}}{s+\alpha} + \kappa = \tau, \tag{2.2}$$

where τ is the total shear stress.

A basic observation about shear flow is that the qualitative dynamics is independent of α. Specifically, if we scale C_{12} with $\sqrt{3+\alpha}$, $C_{11}-1$ with $3+\alpha$, τ with $1/\sqrt{3+\alpha}$, time with $3+\alpha$ and ϵ with $(3+\alpha)^{-2}$,

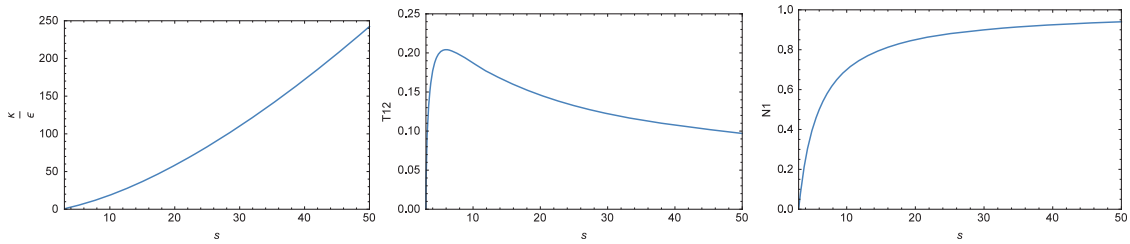

FIG. 2. Shear rate κ/ϵ, shear stress $T_{12,PEC}$ and first normal stress N_1 as given by (2.3) for $\alpha = 0$.

then α scales out of the equations. By contrast, α profoundly influences the qualitative dynamics in elongational flow (see the relevant section below).

2.1. *Steady shear flow*

In steady shear flow, we obtain from the above equations that

$$\begin{aligned} N_1 = T_{11} - T_{22} &= \frac{1}{s+\alpha}(C_{11} - 1) = \frac{s-3}{s+\alpha}, \\ T_{12,\mathrm{PEC}} &= \frac{C_{12}}{s+\alpha} = \frac{1}{s+\alpha}\sqrt{\frac{s-3}{2}}, \\ \frac{\kappa}{\epsilon} &= (s+\alpha)\sqrt{\frac{s-3}{2}}. \end{aligned} \tag{2.3}$$

We note that κ/ϵ and N_1 are monotone functions of s, but $T_{12,\mathrm{PEC}}$ is not. We show a plot for $\alpha = 0$ in Fig. 2. Indeed, the elastic shear stress reaches a maximum value at $s = \alpha + 6$; the value of this maximum is

$$T_M = \frac{1}{2\sqrt{2(3+\alpha)}}. \tag{2.4}$$

As s increases beyond $\alpha+6$, $T_{12,\mathrm{PEC}}$ decreases with increasing s and actually approaches zero as $s \to \infty$. We note that the shear rate value at which $s = \alpha+6$ is reached is proportional to ϵ. As $T_{12,\mathrm{PEC}}$ decreases, the total shear stress goes through a minimum and then increases again, due to the Newtonian contribution. It can be shown, to leading order in ϵ, the value of the shear stress at the minimum is

$$T_m = 2^{3/2}3^{-3/4}\epsilon^{1/4}, \tag{2.5}$$

and the corresponding shear rate is $3^{-3/4}2^{-1/2}\epsilon^{1/4}$.

2.2. *Startup and cessation of shear flow*

In the following, we shall regard the total shear stress τ as given. In startup of steady shear flow, we initially have equilibrium, i.e. $\kappa = 0$, $C_{11} = 1$, $C_{12} = 0$. Starting from $t = 0$, we impose a prescribed

constant shear stress τ. From (2.1) and (2.2), we obtain the system

$$\dot{C}_{11} = 2(\tau - \frac{C_{12}}{s+\alpha})C_{12} - \epsilon(s+\alpha)(C_{11}-1),$$
$$\dot{C}_{12} = \tau - \frac{C_{12}}{s+\alpha} - \epsilon(s+\alpha)C_{12}. \tag{2.6}$$

We can distinguish three distinct dynamical regimes: fast, slow and yielded.

2.2.1. *Fast dynamics* If we simply set $\epsilon = 0$, then the system (2.6) reduces to

$$\dot{C}_{11} = 2(\tau - \frac{C_{12}}{s+\alpha})C_{12},$$
$$\dot{C}_{12} = \tau - \frac{C_{12}}{s+\alpha}. \tag{2.7}$$

We refer to this regime as fast dynamics. We can conclude from (2.7) that

$$C_{11} - C_{12}^2 = K, \tag{2.8}$$

where K is a constant. If the shear flow starts from equilibrium, then $K = 1$. Substitution into the second equation of (2.7), noting that $s = C_{11} + 2$, leads to

$$\dot{C}_{12} = \tau - \frac{C_{12}}{K + 2 + \alpha + C_{12}^2}. \tag{2.9}$$

We note that the function $C_{12} \mapsto C_{12}/(K+2+\alpha+C_{12}^2)$ goes through a maximum when $C_{12}^2 = K+2+\alpha$.

2.2.2. *Slow dynamics* If $\tau < 1/(2\sqrt{K+2+\alpha})$, then fast dynamics can reach an equilibrium point. When this happens, there is a transition to another regime which we call slow dynamics. In slow dynamics, the shear rate κ is small on the same order as ϵ. To obtain a leading order approximation of slow dynamics, we note that

$$\frac{\mathrm{d}}{\mathrm{d}t}(C_{11} - C_{12}^2) = -\epsilon(s+\alpha)(C_{11} - 1 - 2C_{12}^2). \tag{2.10}$$

In this equation, we approximate C_{12} by $\tau(s+\alpha)$. We can further scale out ϵ by setting $\tilde{t} = \epsilon t$. We obtain a single equation, which can be written in terms of s as

$$\frac{\mathrm{d}}{\mathrm{d}t}(s - \tau^2(s+\alpha)^2) = -(s+\alpha)(s - 3 - 2\tau^2(s+\alpha)^2). \tag{2.11}$$

The points of particular interest are equilibrium points and singular points. At equilibrium points, $s - 3 - 2\tau^2(s+\alpha)^2 = 0$. This leads exactly to the equilibrium point for steady shear flow discussed above. At a singular point, we have

$$\frac{\mathrm{d}}{\mathrm{d}s}(s - \tau^2(s+\alpha)^2) = 0, \tag{2.12}$$

i.e. $s+\alpha = 1/(2\tau^2)$. These singular points are points of tangency between the slow curve $C_{12} = \tau(s+\alpha)$ and a fast curve $C_{11} - C_{12}^2 = K$. If the slow dynamics converges to one of these singular points, there is a transition to fast dynamics.

2.2.3. *Yielded dynamics* In yielded dynamics, we cannot neglect the ϵ terms because they are multiplied by a large quantity. Specifically, we set $C_{12} = \epsilon^{-1/3}\hat{C}_{12}$, $C_{11} = \epsilon^{-2/3}\hat{C}_{11}$ and $t = \epsilon^{-1/3}\hat{t}$. With these rescalings, the leading order balance in (2.6) becomes

$$\begin{aligned} \frac{\mathrm{d}}{\mathrm{d}\hat{t}}\hat{C}_{11} &= 2\tau\hat{C}_{12} - \hat{C}_{11}^2, \\ \frac{\mathrm{d}}{\mathrm{d}\hat{t}}\hat{C}_{12} &= \tau - \hat{C}_{11}\hat{C}_{12}. \end{aligned} \tag{2.13}$$

If $\tau > 0$, yielded dynamics has a fixed point in the first quadrant given by $\hat{C}_{11} = 2^{1/3}\tau^{2/3}$. $\hat{C}_{12} = 2^{-1/3}\tau^{1/3}$. Moreover, this fixed point can be shown to be globally attracting with the invariant region $\hat{C}_{11} > \hat{C}_{12}^2$.

2.2.4. *Startup of shear flow* If shear flow is started from equilibrium, fast dynamics (with $K = 1$) describes the initial evolution. The governing equations are given in (2.7). Eventually, either an equilibrium is reached, or the solution will tend to infinity. The former case occurs if

$$\tau < T_e = 1/(2\sqrt{3+\alpha}). \tag{2.14}$$

If τ is larger than this threshold value, then the solution for fast dynamics goes to infinity, and there is a transition to yielded dynamics at a time of order $\epsilon^{-1/3}$ (see Section 2.2.3). Yielded dynamics then reaches an equilibrium. If $\tau < T_e$, fast dynamics reaches equilibrium, and there is a transition to slow dynamics (see Section 2.2.2). During slow dynamics, the shear rate is of order ϵ and the evolution takes place on a slow time scale of order $1/\epsilon$. Eventually, an unyielded steady state is reached if $\tau < T_M$. If, on the other hand, $\tau > T_M$, then there is no equilibrium for slow dynamics. Instead, the solution approaches a singular point. At that point, there is a transition to another fast curve, along which the flow eventually yields.

We note that $T_e = \sqrt{2}T_M$. If τ is between T_M and T_e, there will be unyielded behaviour over short times: the fast dynamics approaches an equilibrium. Over long times, however, the fluid eventually yields. Yielding is delayed, and the delay lengthens as τ approaches T_M. This is the behaviour which is illustrated in Fig. 1.

2.2.5. *Cessation of shear flow* Now suppose we start with an established yielded shear flow and then lower the imposed value of shear stress. If we lower the shear stress to any non-zero value (more precise, to any value large relative to $\epsilon^{1/4}$), then the flow will remain yielded and simply approach a new equilibrium via yielded dynamics. On the other hand, if we lower the imposed shear stress to zero, then the yielded dynamics will approach $\hat{C}_{11} = \hat{C}_{12} = 0$, and at this point there is a transition to slow dynamics. Following slow dynamics, C_{11} relaxes to its equilibrium value of 1 on a time scale of order ϵ^{-1}. On the other hand, the shear rate approaches zero on a much faster time scale; indeed κ is virtually zero for $t >> \epsilon^{-1/2}$ (see Renardy (2010) for details). Suppose we now impose a new shear stress before the fluid has fully relaxed to equilibrium. This sets up a new initial value problem, which initially is described by fast evolution. However, the fast curve that is followed is not the one with $K = 1$, but one

with a larger value of K. Consequently, we observe a much lower yield stress. This phenomenon is what is commonly referred to as thixotropy.

2.3. *A modified PEC model*

A potential flaw of the PEC model is that, in the limit $\epsilon = 0$, the stress threshold for unyielding goes all the way down to zero. This is somewhat ameliorated by the fact that the stress minimum is only of order $\epsilon^{1/4}$ as noted above. Nevertheless, if ϵ is extremely small, it becomes desirable to modify the model and allow a non-zero stress for unyielding. This can be accomplished by modifying the constitutive functions which appear in (1.1) and (1.3). Maki & Renardy (2010, 2012) have investigated a model which leaves ϕ and ψ the same as for PEC, but changes $\chi(s)$ to $(s+\alpha)(1+q(s-3))$, where q is an 'unyielding parameter.' They fitted data for bentonite suspensions with $\epsilon = 10^{-5}$, $\alpha = -2$ and $q = 0.05$. For this modified model, the value of the stress minimum in the limit $\epsilon \to 0$ is equal to $\sqrt{(1-3q)q/2}$ rather than zero.

The analysis of the modified model is significantly more complex than that of the PEC model, although it shows many similarities. The basic asymptotic regimes of fast, slow and yielded dynamics persist. The most striking new feature of qualitative dynamics is that both unyielded and yielded steady shear flows can lose stability to subcritical Hopf bifurcations. If the imposed shear stress falls into the range where this happens, relaxation oscillations result where a solution alternates between a phase of fast yielding and a phase of slow unyielding. Such 'fracture-heal' cycles appear to have been observed in laponite suspensions (Ianni *et al.*, 2008).

2.4. *Oscillatory shear flows*

We now consider an oscillatory imposed shear stress $\tau(t) = B\sin(\omega t)$. This adds another time scale, namely the period of the oscillation $2\pi/\omega$. This time scale should be compared with the relaxation time and retardation time. We are interested in a regime where the ratio of relaxation time to retardation time is large (of order $1/\epsilon$). The behaviour in limiting cases is easily understood. First, if the period of the oscillation is long relative to the relaxation time, then a quasisteady state results: at each instant of time the flow is effectively given by a steady shear flow with the imposed stress $\tau(t)$. If $B > T_M$, then a cycle of yielding and unyielding occurs during each oscillation; if $B < T_M$, then the flow remains unyielded. Secondly if, on the other hand, the period of oscillation is short relative to the retardation time, then there is insufficient time to build up an elastic stress, and the response is dominated by the Newtonian 'solvent' viscosity. Thus the shear rate simply undergoes a sinusoidal oscillation synchronous with that of the shear stress. The interesting range is where the period of the oscillation is intermediate between retardation time and relaxation time. This regime was investigated in recent work by Renardy & Wang (2015).

The flow considered in Renardy & Wang (2015) is stress controlled and homogeneous. In prior literature, the PEC model and a refinement of it, known as the VCM model, were used to analyse large amplitude oscillatory shear flows of wormlike micelles (Dimitriou *et al.*, 2012; Zhou *et al.*, 2010). However, the experimental data addressed there are for prescribed (nominal) strain rather than stress. In prescribed strain experiments, the shear rate becomes inhomogeneous as soon as yielding occurs, and shear bands develop. The analysis of this problem is more complex than the analysis of homogeneous shear flows; we shall return to this point in a later section. Although a direct comparison is not possible, the analysis in Renardy & Wang (2015) explains some qualitative features of the results found in Zhou *et al.* (2010). The parameters used by Zhou *et al.* (2010), in our notation, are $\alpha = 1.286$, $\epsilon = 0.00027$. Stress

controlled experiments on simple yield stress fluids such as Carbopol are in the literature (Dimitriou *et al.*, 2013); analogous experiments on thixotropic yield stress fluids in oscillatory shear are yet to be conducted.

Renardy & Wang (2015) consider an imposed shear stress $\tau = B\sin(\omega t)$. In the non-dimensionalization we have chosen, the retardation time is of order 1, and the relaxation time is of order $1/\epsilon$, so the range of interest is

$$\epsilon < \omega < 1. \tag{2.15}$$

As we have noted above, the qualitative dynamics for shear flows is independent of α; in Renardy & Wang (2015), α has been set equal to 1. We now set $\omega = \epsilon^p$, where $0 < p < 1$, $\omega t = r$ and $u = C_{11} - C_{12}^2$. The system (2.6) then assumes the form

$$\begin{aligned} \frac{\mathrm{d}C_{12}}{\mathrm{d}r} &= \epsilon^{-p}\Big[B\sin(r) - \frac{C_{12}}{C_{12}^2 + u + 3} + O(\epsilon)\Big] \\ \frac{\mathrm{d}u}{\mathrm{d}r} &= \epsilon^{1-p}(C_{12}^2 + u + 3)(1 - u + C_{12}^2). \end{aligned} \tag{2.16}$$

We first consider 'yielded' solutions of the system (2.16). If the amplitude of the sine function exceeds the maximum of the function $C_{12} \mapsto C_{12}/(C_{12}^2 + u + 3)$, then C_{12} grows to a magnitude of order ϵ^{-p}, and the term $C_{12}/(C_{12}^2 + u + 3)$ then becomes small of order ϵ^p. As a result, there is a balance between the derivative $\mathrm{d}C_{12}/\mathrm{d}r$ and $\epsilon^{-p}B\sin r$, and C_{12} oscillates with an amplitude of order ϵ^{-p}. In the second equation of (2.16), we can use an averaging approximation. This leads to a solution, where, to leading order, we have

$$C_{12} = -B\epsilon^{-p}\cos r, \quad u = \epsilon^{-2p}B^2\sqrt{3/8}. \tag{2.17}$$

This approximation is valid as long as the terms denoted by $O(\epsilon)$ in (2.16) remain negligible; this turns out to be the case as long as $p < 1/3$.

This 'yielded' solution exists for any positive B. If B is sufficiently small, however, there is another 'unyielded' solution, where, in the first equation of (2.16), $B\sin r$ is balanced against $C_{12}/(C_{12}^2 + u + 3)$. Averaging can still be applied to the second equation, i.e. to leading order u is constant and satisfies the equation

$$-u^2 - 2u + 3 + 4\langle C_{12}^2\rangle + \langle C_{12}^4\rangle = 0, \tag{2.18}$$

where $\langle\cdot\rangle$ denotes the temporal average. The condition for this unyielded solution to exist is that B does not exceed the maximum of the function $C_{12}/(C_{12}^2 + u + 3)$. If the unyielded solution exists, it is, to leading order, independent of $p \in (0, 1)$. Yielded and unyielded solutions can coexist at the same shear stress, leading to shear bands.

While the unyielded solution, if it exists, persists over the entire range of p, the assumptions used to obtain the yielded solution break down if p exceeds 1/3. In this case, the $O(\epsilon)$ terms indicated in the first equation of (2.16) cannot be neglected any more, and a transition to yielded dynamics occurs. To describe yielded dynamics, we rescale $C_{11} = \epsilon^{-2/3}\tilde{C}_{11}$ and $C_{12} = \epsilon^{-1/3}\tilde{C}_{12}$. The rescaled system, at

leading order, is as follows:

$$\frac{\mathrm{d}}{\mathrm{d}r}\tilde{C}_{11} = \epsilon^{1/3-p}(2B\sin(r)\tilde{C}_{12} - \tilde{C}_{11}^2),$$
$$\frac{\mathrm{d}}{\mathrm{d}r}\tilde{C}_{12} = \epsilon^{1/3-p}(B\sin(r) - \tilde{C}_{11}\tilde{C}_{12}). \tag{2.19}$$

Since $p > 1/3$, we expect a solution which can be approximated by setting the right hand sides equal to zero:

$$0 = 2B\sin(r)\tilde{C}_{12} - \tilde{C}_{11}^2,$$
$$0 = B\sin(r) - \tilde{C}_{11}\tilde{C}_{12}. \tag{2.20}$$

This leads to $\tilde{C}_{12} = (B\sin r/2)^{1/3}$ and $\tilde{C}_{11} = 2^{1/3}(B\sin r)^{2/3}$. The assumption that the left hand side of (2.19) can be neglected becomes inconsistent when $\sin r$ is small on the same order as $\epsilon^{(3p-1)/5}$. At that point, the full system (2.19) must be considered.

This asymptotic regime persists as long as $1/3 < p < 3/4$. When p exceeds 3/4, the oscillation becomes slow enough to allow time for partial unyielding. A detailed description of the asymptotics is quite intricate, and the reader is referred to Renardy & Wang (2015). The yielded dynamics as described in the preceding paragraph prevails when r is not close to a zero of the sine function. Near zeros of the sine function, we have the following stages:

(1) Yielded dynamics breaks down when $n\pi - r$ becomes small of order $\epsilon^{1/4}$. At this point, elastic stresses become of the same order as viscous stresses and must be included in the leading balance. The behaviour remains quasistatic as it was in the yielded regime, i.e. the time derivatives of C_{11} and C_{12} can be neglected. The orders of magnitude of C_{11} and C_{12} are, respectively, $\epsilon^{-1/2}$ and $\epsilon^{-1/4}$ during this stage.

(2) At a critical value $\bar{\sigma}$ of $(n\pi - r)/\epsilon^{1/4}$, the existence of a quasistatic solution is lost. We then enter a new regime of more rapid change, during which $r = n\pi - \bar{\sigma}\epsilon^{1/4} + O(\epsilon^{p-1/2})$. During this phase, C_{11} and C_{12} decrease to order of magnitude $\epsilon^{p-5/4}$ and ϵ^{p-1}, respectively.

(3) This is followed by a phase of slow evolution, during which the shear rate is negligible, i.e. to leading order $\tau = B\sin r$ is balanced by the elastic stress $C_{12}/(C_{11}+3)$. During this phase, C_{11} is slowly decreasing. This phase persists until $r - n\pi$ is of order ϵ^{1-p}. At this point, C_{11} has decreased to the order of magnitude ϵ^{2p-2}.

(4) Finally, there is a yielding phase which occurs over a short time scale. At the end of this phase, the system returns to yielded dynamics.

One of the crucial aspects in understanding these results is that yielding happens on a faster time scale than unyielding. For a stress amplitude of order 1, a period of order $\epsilon^{-1/3}$ is long enough to allow full unyielding and a transition to yielded dynamics. On the other hand, a much longer period of order $\epsilon^{-3/4}$ is needed before any unyielding occurs.

3. Elongational flows

The PEC and related models have been applied successfully to interpret elongational flows in wormlike micelles, see Cromer *et al.* (2009). One of the most striking findings in such flows is a significant

difference between uniaxial and biaxial extension (Rothstein, 2008; Walker *et al.*, 1996): extensional thickening is observed in uniaxial extension but not in biaxial extension. Wormlike micelles have a yield stress that is relatively high compared to the stress modulus; this allows some elongational deformation before yielding occurs. For fluids with a low yield stress, on the other hand, it is difficult to set up an elongational flow, and there are few if any data. There are some measurements of yield stress values, which suggest a von Mises criterion correlating yield stress values in elongation to yield stress values in shear (Shaukat *et al.*, 2012); the PEC model is consistent with this (for 'fast' yielding) if α is close to -3 (Grant & Renardy, 2015).

Renardy & Grant (2013) and Grant & Renardy (2015) have studied the startup and cessation of elongational flow of the PEC model in a manner analogous to the analysis of shear flow described above. In elongational flow, the velocity gradient has the form

$$\nabla \mathbf{v} = \begin{pmatrix} \kappa & 0 & 0 \\ 0 & -\frac{\kappa}{2} & 0 \\ 0 & 0 & -\frac{\kappa}{2} \end{pmatrix}, \tag{3.1}$$

and the conformation tensor $\mathbf{C}$ has the form

$$\mathbf{C} = \begin{pmatrix} C_{11} & 0 & 0 \\ 0 & C_{22} & 0 \\ 0 & 0 & C_{22} \end{pmatrix}. \tag{3.2}$$

The flow is uniaxial if $\kappa > 0$ and biaxial if $\kappa < 0$. The imposed elongational stress is given by

$$\tau = T_{11} - T_{22} = 3\kappa + \frac{C_{11} - C_{22}}{s + \alpha}, \tag{3.3}$$

where $s = C_{11} + 2C_{22}$. The flow is uniaxial if $\tau > 0$ and biaxial if $\tau < 0$.

The dynamics of the PEC model is now described by

$$\begin{aligned} \frac{\mathrm{d}C_{11}}{\mathrm{d}t} &= 2\kappa C_{11} + \epsilon(s + \alpha)(1 - C_{11}), \\ \frac{\mathrm{d}C_{22}}{\mathrm{d}t} &= -\kappa C_{22} + \epsilon(s + \alpha)(1 - C_{22}), \\ \kappa &= \frac{1}{3}(\tau - \frac{C_{11} - C_{22}}{s + \alpha}). \end{aligned} \tag{3.4}$$

3.1. *Steady elongational flow*

In steady elongational flow, it can be shown that κ/ϵ and s are related by the quadratic equation

$$2(\frac{\kappa}{\epsilon})^2 s + \frac{\kappa}{\epsilon}(s - 3)(s + \alpha) + (3 - s)(s + \alpha) = 0. \tag{3.5}$$

For any $s > 3$, this equation has a positive solution κ/ϵ corresponding to uniaxial flow and a negative solution corresponding to biaxial flow. We find

$$\frac{\kappa}{\epsilon} = -\frac{s + \alpha}{4s}(\mp\sqrt{3(s - 3)(3s - 1)} + s - 3). \tag{3.6}$$

The corresponding elongational stress is

$$\tau = 3\kappa + \frac{s - 3 \pm \sqrt{3(s-3)(3s-1)}}{4(s+\alpha)}. \tag{3.7}$$

In contrast to shear flow, the dependence of τ on κ is non-monotone only if α is sufficiently negative. Specifically, it is shown in Renardy & Grant (2013) and Grant & Renardy (2015) that non-monotone dependence of elongational stress on elongation rate arises in uniaxial flow if $\alpha < -2$ and in biaxial flow if $\alpha < -1$.

3.2. *Fast, slow and yielded dynamics*

We now consider the transient dynamics for startup or cessation of flow. As in the case of shear flow, we can distinguish distinct regimes of fast, slow and yielded dynamics.

In fast dynamics, we neglect the ϵ terms in (3.4). As a result, we have

$$\begin{aligned} \frac{\mathrm{d}C_{11}}{\mathrm{d}t} &= 2\kappa C_{11}, \\ \frac{\mathrm{d}C_{22}}{\mathrm{d}t} &= -\kappa C_{22}, \\ \kappa &= \frac{1}{3}(\tau - \frac{C_{11} - C_{22}}{s+\alpha}). \end{aligned} \tag{3.8}$$

We conclude that $C_{11}C_{22}^2$ is equal to a constant K. By setting $C_{11} = K/C_{22}^2$ and using the last equation of (3.8) to express κ, we find a single equation for the evolution of C_{22}.

In slow dynamics, κ is close to zero (of order ϵ). We can deduce from (3.4) that

$$\frac{\mathrm{d}}{\mathrm{d}t}(C_{11}C_{22}^2) = -\epsilon C_{11}C_{22}^2(s+\alpha)(3 - \frac{1}{C_{11}} - \frac{2}{C_{22}}). \tag{3.9}$$

The equation for slow dynamics is obtained by setting $\kappa = 0$, which yields a relationship between C_{11} and C_{22}, resulting in a single equation for C_{22}.

In yielded dynamics, either C_{11} (in uniaxial extension) or C_{22} (in biaxial extension) is of order $1/\epsilon$. For instance, if we assume uniaxial extension and set $C_{11} = \epsilon^{-1}\tilde{C}_{11}$, then to leading order (3.4) reduces to

$$\begin{aligned} \frac{\mathrm{d}\tilde{C}_{11}}{\mathrm{d}t} &= 2\kappa\tilde{C}_{11} - \tilde{C}_{11}^2, \\ \frac{\mathrm{d}C_{22}}{\mathrm{d}t} &= -\kappa C_{22} + \tilde{C}_{11}(1 - C_{22}), \\ \kappa &= \frac{1}{3}(\tau - 1). \end{aligned} \tag{3.10}$$

In the biaxial case, we find instead

$$\frac{\mathrm{d}C_{11}}{\mathrm{d}t} = 2\kappa C_{11} + 2\tilde{C}_{22}(1 - C_{11}),$$
$$\frac{\mathrm{d}C_{22}}{\mathrm{d}t} = -\kappa \tilde{C}_{22} - 2\tilde{C}_{22}^2,$$
$$\kappa = \frac{1}{3}\left(\tau + \frac{1}{2}\right). \tag{3.11}$$

3.3. *Startup and cessation of elongational flow*

The analysis of startup and cessation of elongational flow is similar to that of shear flow, but the details are considerably more complicated. We refer to Renardy & Grant (2013) and Grant & Renardy (2015) for the specifics, and merely give a brief summary of the results. The initial dynamics starting from equilibrium always follows a fast curve. If $\tau < 1$ for uniaxial extension or $\tau > -1/2$ for biaxial extension, then the initial fast curve reaches equilibrium, and there is a transition to slow dynamics, ultimately leading to an unyielded steady flow.

If, on the other hand, $\tau > 1$ or $\tau < -1/2$, and $\alpha > 0$, then there is a transition to yielded dynamics, leading to a yielded steady flow. A more complicated scenario arises when $\alpha < 0$. In this case, fast yielding occurs only if

$$\alpha > \frac{3(1-\tau)^{1/3}}{\tau}\left(\frac{2\tau+1}{2}\right)^{2/3}. \tag{3.12}$$

If α is less than this threshold value, the fast dynamics reaches equilibrium, and there is a transition to slow dynamics. If an unyielded steady flow exists at the given values of α and τ, the slow dynamics will converge to that state. If not, then there is delayed yielding, i.e. the slow dynamics approaches a singularity, and then there is transition to yielding along another fast curve. We note that the critical value of α given by (3.12) approaches zero when $\tau = 1$ or $\tau = -1/2$, but approaches -3 if $|\tau| \to \infty$. The upper curve in each of the plots in Fig. 3 shows the critical value of α as given by (3.12) in uniaxial and biaxial flow. In the region below the upper curve, the flow transitions to slow dynamics. Steady

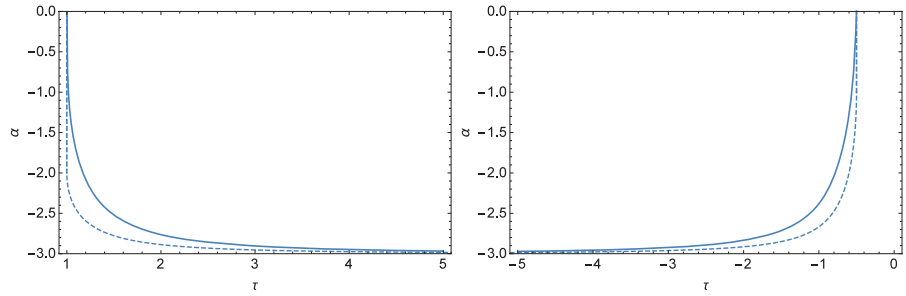

FIG. 3. Critical value of α as given by (3.12) (solid curve) and existence boundary for steady unyielded flow (dashed curve) for uniaxial (left) and biaxial (right) extension.

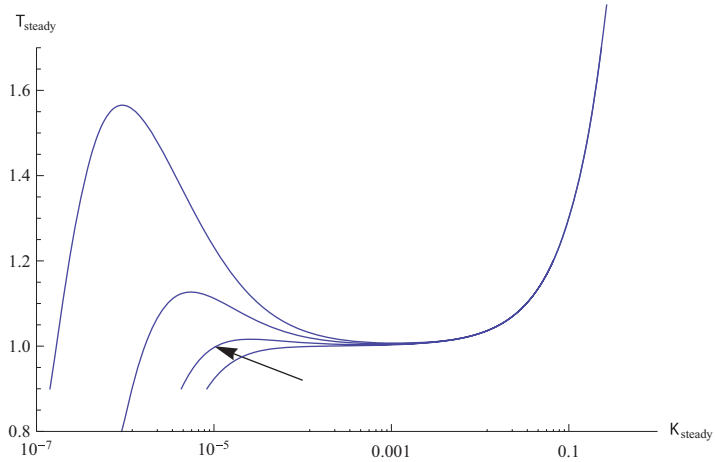

FIG. 4. Steady elongational flow curves for $\alpha = -2$, -2.2, -2.5 and -2.8. The value of α is decreasing from right to left. Reproduced from Fig. 1b of Renardy & Grant (2013).

unyielded flows exist below the lower curve. In the parameter region between the two curves, there is delayed yielding. Figure 4 shows the steady flow curve in uniaxial flow. Non-monotone behaviour exists only if $\alpha < -2$.

The behaviour in elongational flow is thus quite different from that in shear. In particular, non-monotonicity and delayed yielding do not occur for $\alpha > 0$, i.e. in the range relevant to wormlike micelles. The unyielding behaviour is also different. If we start from an established yielded flow and then lower the imposed stress, then we saw above that (in the limit $\epsilon \to 0$) we have to lower the stress all the way to zero for shear flows. In elongational flow, on the other hand, unyielding will occur if $|\tau|$ is lowered below 1 (uniaxial case) or 1/2 (biaxial case). Unyielding occurs via slow dynamics, resulting in thixotropic behaviour as in shear flow.

4. Future directions: inhomogeneous flows and shear banding

The flows considered so far have all been assumed spatially homogeneous. If the flow is not homogeneous, then yielded and unyielded regions may coexist, and different asymptotic regimes of fast, slow and yielded dynamics will apply in different regions of space, with moving boundaries. In general, the asymptotic description of solutions can be expected to become quite complicated. The resolution of this problem poses a future challenge.

Perhaps the simplest situation for a spatially inhomogeneous flow is a pressure-driven Poiseuille flow. Let us say the flow is in the x-direction, in the channel $-1 < y < 1$, τ denotes the shear stress, and P_x is the given pressure gradient. If creeping flow is assumed, we have the stress balance $\tau_y = P_x$, i.e. we find $\tau = P_x y$. For each y, we then have a problem of shear flow with prescribed stress as was discussed above. However, the dependence on y raises new questions for asymptotic analysis.

Consider startup of Poiseuille flow, i.e. the fluid is initially at rest, and the pressure gradient is imposed starting at $t = 0$. We assume $P_x > T_e$, where T_e is as in Section 2.2.4 above. We know from the discussion of startup of shear flow above that there will be fast yielding for $|\tau| > T_e$, i.e. $|y| > T_e/P_x$, delayed yielding for $T_M/P_x < |y| < T_e/P_x$, and unyielded flow for $|y| < T_M/P_x$. The transition between

TABLE 1 *Yield time and width of yield zone as a function of shear stress*

Value of τ	Yield time	Width of yield zone
$\frac{1}{4}+\delta, \delta >> \epsilon^{2/3}$	$\delta^{-1/2}$	$\delta^{3/2}$
$\frac{1}{4}+\delta, \delta = O(\epsilon^{2/3})$	$\epsilon^{-1/3}$	ϵ
$\frac{1}{4}-\delta, \delta >> \epsilon^{2/3}$	$\delta\epsilon^{-1}$	ϵ
Between $1/(4\sqrt{2})$ and $1/4$	ϵ^{-1}	ϵ
$\tau_m+\delta, \delta > 0$	$\epsilon^{-1}\delta^{-1/2}$	$\epsilon\delta^{3/2}$

yielded and unyielded regions moves inward and sharpens as time progresses. How do the location and width of this transition zone depend on time? In Renardy & Wang (2015) we address this question. The results are summarized in Table 1. We have set $\alpha = 1$, so that $T_e = 1/4$ and $T_M = 1/(4\sqrt{2})$. τ_m is the stress maximum in steady shear flow, which is equal to T_M plus a correction of order ϵ.

In viscometric devices, the shear stress is not perfectly homogeneous, due to imperfections of the device. If the imposed shear stress falls in the region where delayed yielding occurs, transient shear bands can form. All of the fluid eventually yields, but the yield time varies across the sample. See Moorcroft & Fielding (2013) for an analysis of this phenomenon for the Rolie–Poly model, which behaves in a similar way as the PEC.

As time tends to infinity, the shear banding transition becomes infinitely sharp. Also, the transition may occur at any stress level between the minimum and maximum of stress in the steady flow curve, depending on flow history. These features change if regularizing effects are included in the analysis. This adds another small parameter to the analysis. The idea is to include effects which are usually negligible, but need to be taken into account if there is a large gradient in the shear rate. Such effects will lead not only to a smoothing of the transition, but will also determine the ultimate location and stress level at which the transition occurs. Stress diffusion has been widely used as a regularizing mechanism, see Fardin *et al.* (2012), Lu *et al.* (2000), Spenley *et al.* (1996) and Zhou *et al.* (2012). Stress diffusion is motivated by theories of dilute polymer solutions, where polymer molecules diffuse in a Newtonian solvent and take their stresses with them. The molecular structure of fluids in which shear banding actually occurs, however, tends to be quite different. Recent work by one of us suggested a different mechanism, based on Korteweg stresses which result from an interfacial energy, which can, for instance, be motivated as a tube mismatch energy in theories of entangled polymers (see Renardy, 2014). With either stress diffusion or Korteweg stresses, there is now a second small parameter in addition to ϵ. A systematic investigation of the asymptotics generated by the interplay of these two parameters remains as a challenge for the future.

Funding

National Science Foundation under Grant DMS-1311707.

REFERENCES

BARNES, H. A. & WALTERS, K. (1985) The yield stress myth? *Rheol. Acta*, **24**, 323–326.

BARNES, H. A. (1999) The yield stress– a review, or '$\pi\alpha\nu\tau\alpha\ \rho\epsilon\iota$'– everything flows. *J. Non-Newtonian Fluid Mech.*, **81**, 133–178.

CATON, F. & BARAVIAN, C. (2008), Plastic behavior of some yield stress fluids: from creep to long-time yield. *Rheol. Acta*, **47**, 601–607.

CHENG, D. C.-H. (1986) Yield stress: a time dependent property and how to measure it. *Rheol. Acta*, **25**, 542–554.

COUSSOT, P. & GAULARD, F. (2005) Gravity flow instability of viscoplastic materials: the ketchup drip. *Phys. Rev. E*, **72**, 031409.

COUSSOT, P. (2014) *Rheophysics.* Cham, Switzerland: Springer International Publishing.

CROMER, M., COOK, L. & MCKINLEY, G. H. (2009) Extensional flow of wormlike micellar solutions. *Chem. Eng. Sci.*, **64**, 4588–4596.

DIMITRIOU, C., CASANELLAS, L., OBER, T. J. & MCKINLEY, G. H. (2012) Rheo-PIV of a shear-banding wormlike micellar solution under large amplitude oscillatory shear. *Rheol. Acta*, **51**, 395–411.

DIMITRIOU, C., EWOLDT, R. & MCKINLEY, G. H. (2013) Describing and prescribing the constitutive response of yield stress fluids using large amplitude oscillatory shear stress (LAOStress). *J. Rheol.*, **57**, 27–70.

FARDIN, M. A., OBER, T. J., GAY, C., GRÉGOIRE, G., MCKINLEY, G. H. & LEROUGE, S. (2012) Potential "ways of thinking" about the shear-banding phenomenon. *Soft Matter*, **8**, 910–922.

FIELDING, S. M. (2009) Shear banding, aging and noise dynamics in soft, glassy materials. *Soft Matter*, **5**, 2378–2382.

GRANT, H. V. & RENARDY, Y. (2015) Equibiaxial extension of a viscoelastic partially extending strand convection model with large relaxation time. *Rheol. Acta*, **54**, 563–579.

IANNI, F., DI LEONARDO, R., GENTILINI, S. & RUOCCO, G. (2008) Shear-banding phenomena and dynamical behavior in a laponite suspension. *Phys. Rev. E*, **77**, 031406.

JAMES, A. E., WILLIAMS, D. J. A. & WILLIAMS, P. R. (1987) Direct measurement of static yield properties of cohesive suspensions. *Rheol. Acta*, **26**, 437–446.

LARSON, R. G. (1984) A constitutive equation for polymer melts based on partially extending strand convection. *J. Rheol.*, **28**, 545–571.

LU, C.-Y. D., OLMSTED, P. D. & BALL, R. C. (2000) Effects of non-local stress on the determination of shear banding flow. *Phys. Rev. Lett.*, **84**, 642–645.

MAKI, K. L. & RENARDY, Y. (2010) The dynamics of a simple model for thixotopic yield stress fluids. *J. Non-Newtonian Fluid Mech.*, **165**, 1373–1385.

MAKI, K. L. & RENARDY, Y. (2012) The dynamics of a viscoelastic fluid which displays thixotopic yield stress behavior. *J. Non-Newtonian Fluid Mech.*, **181–182**, 30–50.

MEWIS, J. & WAGNER, N. J. (2013) *Suspension Rheology.* Cambridge: Cambridge University Press.

MOORCROFT, R. L. & FIELDING, S. M. (2013) Criteria for shear banding in time-dependent flows of complex fluids. *Phys. Rev. Lett.*, **110**, 086001.

MØLLER, P. C. F, MEWIS, J. & BONN, D. (2006) Yield stress and thixotropy: on the difficulty of measuring yield stresses in practice. *Soft Matter*, **2**, 274–283.

NGUYEN, Q. D. & BOGER, D. V. (1992) Measuring the flow properties of yield stress fluids. *Ann. Rev. Fluid Mech.*, **24**, 57–88.

PICARD, G., AJDARI, A., BOCQUET, L. & LECQUEUX, F. (2002) Simple model for heterogeneous flows of yield stress fluids. *Phys. Rev. E*, **66**, 051501, 1–12.

RENARDY, M. (2010) The mathematics of myth: yield stress behavior as a limit of nonmonotone constitutive theories, *J. Non-Newtonian Fluid Mech.*, **165**, 519–526.

RENARDY, M. (2014) Korteweg stresses and admissibility criteria for shear banded flows, *J. Non-Newtonian Fluid Mech.*, **213**, 68–72.

RENARDY, M. & WANG, T. (2015) Large amplitude oscillatory shear flows for a model of a thixotropic yield stress fluid. *J. Non-Newtonian Fluid Mech.*, **222**, 1–17.

RENARDY, M. & WANG, T. (2015) Development of shear bands for a model of a thixotropic yield stress fluid. *J. Non-Newtonian Fluid Mech.* (submitted).

RENARDY, Y. & GRANT, H. V. (2013) Uniaxial extensional flow of a thixotropic yield stress fluid: a viscoelastic model, *Rheol. Acta*, **52**, 867–879.

ROTHSTEIN, J. P. (2008) Strong flows of viscoelastic wormlike micelle solutions. *Rheology Reviews*, **2008**, 1–46.

SHAUKAT, A., KAUSHAL, M., SHARMA, A. & JOSHI, Y. M. (2012) Shear mediated elongational flow and yielding in soft glassy materials. *Soft Matter*, **8**, 10107–10114.

SPENLEY, N. E., YUAN, X. F. & CATES, M. E. (1996) Nonmonotonic constitutive laws and the formation of shear-banded flows. *J. Physique II,* **6**, 551–571.

STOKES, J. R. & TELFORD, J. H. (2004) Measuring the yield behaviour of structured fluids. *J. Non-Newtonian Fluid Mech.*, **124**, 137–146.

WALKER, L. M., MOLDENAERS, P. & BERRET, J. F. (1996) Macroscopic response of wormlike micelles to elongational flow. *Langmuir*, **12**, 6309–6314.

ZHOU, L., VASQUEZ, P. A., COOK, L. P. & MCKINLEY, G. H. (2008) Modeling the inhomogeneous response and formation of shear bands in steady and transient flows of entangled liquids. *J. Rheol.*, **52**, 591–623.

ZHOU, L., COOK, L. P. & MCKINLEY, G. H. (2010) Probing shear-banding transitions of the VCM model for entangled wormlike micellar solutions using large amplitude oscillatory shear (LAOS) deformations. *J. Non-Newtonian Fluid Mech.*, **165**, 1462–1472.

ZHOU, L., COOK, L. P. & MCKINLEY, G. H. (2012) Multiple shear-banding transitions for a model of wormlike micellar fluids. *SIAM J. Appl. Math.*, **72**, 1192–1212.